Growth and Characterization of GaSb-Based Type-Ⅱ InAs/GaSb Superlattice Photodiodes for Mid-Infrared Detection *

WANG Guo-Wei(王国伟)[1**], XU Ying-Qiang(徐应强)[1], GUO Jie(郭杰)[2], TANG Bao(汤宝)[1], REN Zheng-Wei(任正伟)[1], HE Zhen-Hong(贺振宏)[1], NIU Zhi-Chuan(牛智川)[1]

[1]*State Key Laboratory for Superlattices and Microstructures, Institute of Semiconductors, Chinese Academy of Sciences, Beijing 100083*

[2]*Luoyang Opti-electronics Development Center, Luoyang 471009*

(Received 28 January 2010)

InAs/GaSb superlattice (SL) midwave infrared photovoltaic detectors are grown by molecular beam epitaxy on GaSb(001) residual p-type substrates. A thick GaSb layer is grown under the optimized growth condition as a buffer layer. The detectors containing a 320-period 8ML/8ML InAs/GaSb SL active layer are fabricated with a series pixel area using anode sulfide passivation. Corresponding to 50% cutoff wavelengths of 5.0 μm at 77 K, the peak directivity of the detectors is 1.6×10^{10} *cm·Hz*$^{1/2}$ *W*$^{-1}$ *at 77 K.*

PACS: 73. 21. Cd, 78. 20. Bh DOI: 10.1088/0256-307X/27/7/077305

Photodetectors in the mid-infrared wavelength range (MWIR) (3–5 μm) have applications in high-speed infrared (IR) imaging for medical applications (diagnosis assistance), industrial applications (pollution monitoring and process control), teledetection by satellites (meteorology and urbanism studies) and defense applications (night vision). An alternative to the HgCdTe and InSb dominated material technologies in this range could be the InAs/GaSb superlattice (SL). This system was first proposed by Smith and Mailhiot for IR detection at the end of the 1980s[1] and has recently emerged as the most promising material system for third-generation IR detectors. Consequently, different groups today devote increasing efforts to the study of InAs/GaSb SL for MWIR detection. Several published results have shown that high quality short period SL structures with very good spatial uniformity can be grown on GaSb substrates with the ability to span cut-off wavelength by varying only the thickness of the InAs and GaSb layers.[2–5] High resolution focal plane array cameras operating at 77 K have been fabricated allowing fast and accurate detection of CO_2 in the MWIR domain by using a dual-color detector.[6–8]

In this Letter, we report GaSb-based midwave wavelength infrared InAs/GaSb SL detectors grown by molecular beam epitaxy (MBE). The crucial issue for the growth of InAs/GaSb SLs on GaSb substrates is to produce a high-quality buffer layer and elaborate perfectly strain-compensated structures to avoid strain relaxation that will induce a degradation of the SL optical and electrical properties.[9–10]

Samples were grown by MBE in a VG80-H system on undoped (100)-GaSb residual p-type substrates with 2″ diameter. The system is equipped with group-Ⅲ SUMO effusion cells for gallium, aluminum and indium and valved cracker cells for arsenic and antimony. Silicon and GaTe as well as beryllium can be used for n- and p-type doping.

In this work, a GaSb buffer layer was growth under an optimized pre-growth preparation and growth condition to decrease the occurrence of bulk defects which maintain a similar pyramidal structure. Included are investigations of pre-growth oxide desorption, GaSb buffer growth temperature, and Sb/Ga ratio during superlattice growth.[11] Figure 1(a) shows an atomic force micrograph (AFM) of a typical surface morphology of 500 nm GaSb grown on GaSb with clear atomic steps and a $10 \times 10\,\mu m^2$ area with an rms roughness of 0.163 nm.

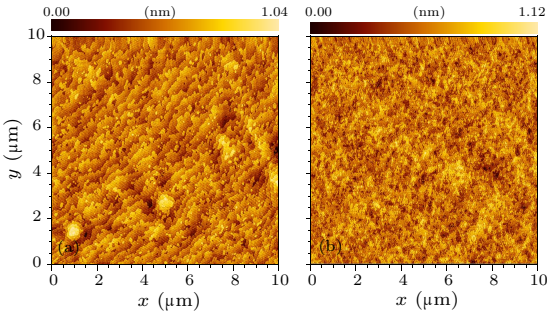


Fig. 1. Surface AFM cartography. (a) A $10 \times 10\,\mu m$ scan area of 500 nm GaSb buffer layer. (b) A $10 \times 10\,\mu m$ scan area of the 500 nm GaSb buffer layer and 320 period superlattices.

The detector structure consists of a p-doped GaSb contact layer ($p \sim 1 \times 10^{18}\,cm^{-3}$), 320 periods of

*Supported by the National Natural Science Foundation of China under Grant No 60625405, and the National Basic Research Program of China under Grant Nos 2007CB936304 and 2010CB327601.

**Email: wangguowei@semi.ac.cn

© 2010 Chinese Physical Society and IOP Publishing Ltd

an InAs/GaSb SL built with 8 monolayer (ML) thick InAs layers and 8ML thick GaSb layers and a 20-nm-thick n-doped InAs cap layer. The lower part of the SL is p-type doped ($p \sim 1\times10^{18}\,\mathrm{cm}^{-3}$ Be in the GaSb layers), followed by an undoped region and an n-type doped stack on top of the structure ($n \sim 1\times10^{18}\,\mathrm{cm}^{-3}$ with Si in the InAs layers).

The properties of type-Ⅱ InAs/GaSb superlattices should be strongly dependent on the interface type. Interfaces have been proposed as a design tool for short period InAs/GaSb superlattices for mid-infrared detectors.[12] Only InSb and GaAs types of interfaces have been experimentally exploited before, but there are limitations in applying only InSb or GaAs interfaces. In order to have almost zero lattice mismatches (well below 1000 ppm), there exist only a certain number of thickness combinations of InAs and GaSb. We use the modified sp3s* empirical tight-binding method (ETBM) and mixed interfaces (IF) of Ga_xIn_{1-x} type[13] to model the superlattice material. At the transition from GaSb to InAs or from InAs to GaSb layers, both group-Ⅲ and group-V elements are changed and the interface compositions depend on the shutter sequence during MBE growth in our MBE system.[14] Figure 2 shows the ETBM modeled bandgap diagram of the 8 ML InAs/8 ML GaSb superlattices with the variation of two interface compositions. In the almost zero lattice mismatch range (below 1000 ppm) the band gap of 8 ML InAs/8 ML GaSb superlattices is in the range of 4.8–5.0 μm.

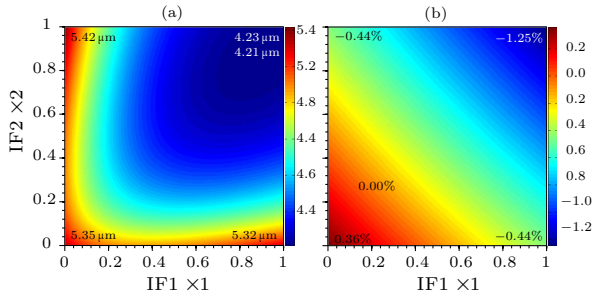


Fig. 2. Sp3s* ETBM Model of $[(AsIn)_7\text{-}AsGa_{x1}In_{1-x1}\text{-}(SbGa)_7\text{-}SbGa_{x2}In_{1-x2}]_N$: (a) Interface bandgap diagram of 8 ML InAs/8 ML GaSb superlattices. (b) Superlattice mismatch diagram of 8 ML InAs/8 ML GaSb superlattices.

During the superlattices growth procedure, growth temperature, V/Ⅲ ratios and shutter sequences have been optimized in order to improve material quality and to establish a manufacturable growth process. Growth rates for both GaSb and InAs were set to 0.513 ML/s and 0.168 ML/s, respectively. InAs V/Ⅲ-flux ratio 10 and GaSb V/Ⅲ-flux ratio 3, formations of Ga_xIn_{1-x} interfaces at the InAs/GaSb and the GaSb/InAs interfaces were forced by the shutter sequence during epitaxy in order to match the tensile strain of the InAs.[10] The best morphological and optical properties were obtained for a substrate temperature of 420°C. The growth temperature was calibrated with the (1×3) to (2×5) GaSb surface reconstruction transition.[15] Figure 3 shows the high-resolution x-ray diffraction and dynamical simulation pattern around the (004) reflection of a standard 30 period mid-IR superlattice structure. The SL has a periodic width of 50.53 Å±2.30 Å and is under compression strain with a residual strain of 72.9 s ($\Delta a/a = 0.063\%$). The full width at half maximum (FWHM) of the GaSb buffer and the first order superlattices are 51.71 and 135.2 arcsec. The diffraction pattern reveals well-resolved satellite peaks up to the sixth order, demonstrating good morphological quality. Figure 1(b) shows an atomic force micrograph (AFM) of 1.6 μm thick MWIR superlattices on the GaSb template; the rms roughness equals 0.280 nm.

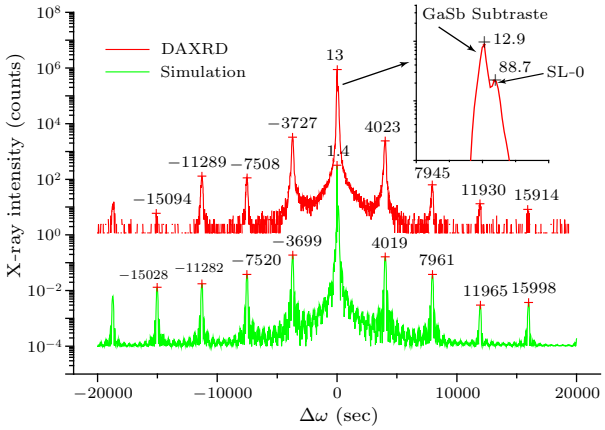


Fig. 3. X-ray diffractometry (004 reflection) of an InAs/GaSb superlattice diode with a total number of 30 periods and the simulation result.

Single element detectors with areas of 100 μm × 100 μm, 200 μm × 200 μm, 400 μm × 400 μm, 800 μm × 800 μm were fabricated by standard lithography and subsequent etching by tartaric acid solution. Top and bottom metal contacts were formed using electron beam deposited Ti/Au. Figure 4(a) shows that the device leakage current density of these photosensitive units under anodic sulfide does not increase obviously with the reduction of detector area at 77 K. This shows that the contribution of surface leakage current is very low. Figure 4(b) shows that the differential resistance and R_0A of PIN diodes achieve $10^3\,\mathrm{A\cdot cm}^2$ in order of magnitude.

Figure 5 shows the positive small bias voltage $I-V$ curves. Under uncompleted dark-field, the detector shows 0.05 V threshold voltage. This is because of the contribution of photocurrent. Under completed dark-field, the leakage current decreases five times. The two subplots in Fig. 5 show the linear fitting of

the two parts of a detector $I-V$ curve. We obtain an ideality factor in the range of 1.5 to 2.1. Thus the generation-recombination current and temperature-insensitive defect-related leakage are the dominant leakage in the depletion region. Reducing the defect density in the depletion region will improve the detector detectivity.[16]

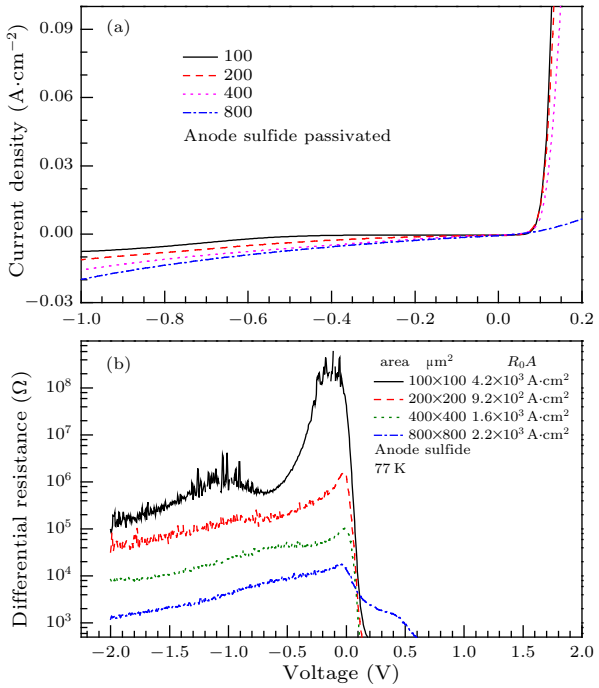


Fig. 4. (a). $I-V$ characteristics of InAs/GaSb superlattice pin photodiodes with different sized areas after anode sulfide passivation (b). The relation between Rdiff and voltage in the pin photodiode after anode sulfide passivation at 77 K.

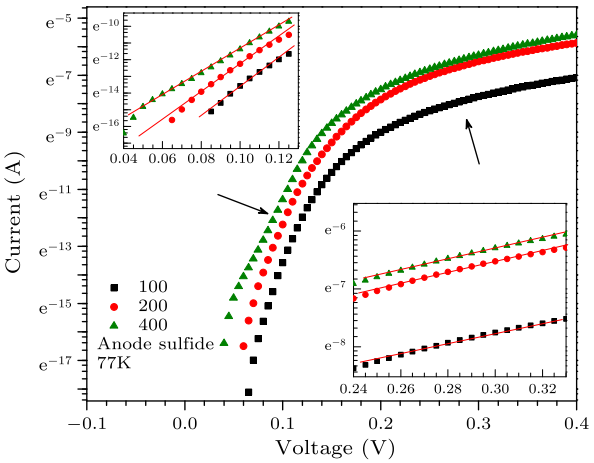


Fig. 5. $\ln I$ versus V for different sized photodiodes after anode sulfide passivation.

The spectral response of the devices was measured with a Fourier transform infrared (FTIR) system. The average detectivity of the mid-wavelength detector based on InAs(8 ML)/GaSb(8 ML) SL was tested with 1.2 mA current under a blackbody temperature of 500 K.

Figure 6 shows the relative photoresponse spectra of the detector at 77 K. The cutoff wavelength (defined as the point where the photoresponse drops to 50% of the maximum value) is 5.0 μm at 77 K. This result is matched to the ETBM-calculated possible to be almost zero lattice mismatches of the superlattice bandgap. In the devices with anode sulfide passivation and ZnS passivation, noise is reduced. The blackbody peak detectivity is 1.6×10^{10} cm·Hz$^{1/2}$/W at 77 K, responsivity 0.06 A/W. This is due to the reduction of surface leakage current and increase of R_0A.

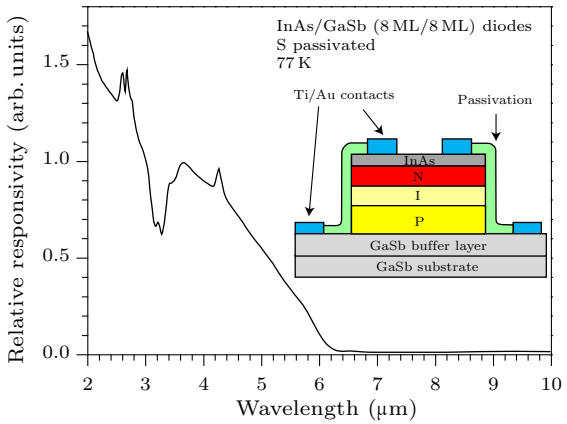


Fig. 6. Photoresponse spectra of the 8 MLs-InAs/8 MLs-GaSb superlattice photodiode at 77 K schematic of the InAs/GaSb SL photodetector.

In summary, InAs/GaSb SLs with broken gap-type-Ⅱ band alignment have been grown by molecular beam epitaxy for the fabrication of mid-IR detection. The p-type GaSb buffer layer and superlattice active region are growth under optimized conditions. The structural and optical properties of type-Ⅱ InAs-GaSb SLs have been studied by HRXRD and AFM. High quality strain-balanced SL structures of 8 MLs-InAs/8 MLs-GaSb have been obtained by formation of Ga_xIn_{1-x} type interfaces. The peak detectivity of the photovoltaic detectors at 50% cutoff wavelength 5.0 μm is 1.6×10^{10} cm·Hz$^{1/2}$w^{-1} at 77 K. $I-V$ curves show that generation-recombination current and temperature insensitive defect-related leakages are the dominant leakage in the depletion region. Thus this InAs/GaSb superlattice detector system will have a much better performance after improving the growth condition and device structure.

References

[1] Smith D L and Mailhiot C 1990 *Rev. Mod. Phys.* **62** 173
[2] Delaunay P Y, Nguyen B M, Hoffman D, Huang E K W and Razeghi M 2009 *IEEE J. Quantum Electron.* **45** 157
[3] Huang E K, Hoffman D, Nguyen B M, Delaunay P Y and

Razeghi M 2009 *Appl. Phys. Lett.* **94** 053506
[4] Nathan V and Razeghi M 2007 *Proc. SPIE* **6542** 654209
[5] Nguyen B M, Hoffman D, Huang E K, Delaunay P Y and Razeghi M 2008 *Appl. Phys. Lett.* **93** 123502
[6] Cabanski W, Eberhardt K, Rode W, Wendler J, Ziegler J, Fleissner J, Fuchs F, Rehm R, Schmitz J, Schneider H and Walther M 2004 *Proc. SPIE* **5406** 184
[7] Cabanski W, Munzberg M, Rode W, Wendler J, Ziegler J, Fleissner J, Fuchs F, Rehm R, Schmitz J, Schneider H and Walther B 2005 *Proc. SPIE* **5783** 340
[8] Rehm R, Schmitz J, Fleissner J, Walther M, Ziegler J, Cabanski W and Breiter R 2005 *Phys. Status Solidi* C **3** 435
[9] Lew A Y, Zuo S L, Yu E T and Miles R H 1997 *Appl. Phys. Lett.* **70** 75
[10] Rodriguez J B, Christol P, Cerutti L, Chevrier F and Joullie A 2005 *J. Cryst. Growth* **274** 6
[11] Aifer E H, Jackson E M, Bennett B R, Vurgaftman I, Meyer J R and Jernigan G G 2002 *Mater. Devices Optoelectron. Microphoton.* **722** 275
[12] Szmulowicz F, Haugan H J, Brown G J, Mahalingam K, Ullrich B, Munshi S R and Grazulis L 2006 *Opto-Electronics Review* **14** 71–77
[13] Yajun W and Razeghi M 2004 *Phys. Rev.* B **69** 085316
[14] Feenstra R M, Collins D A, Ting D Z Y, Wang M W and McGill T C 1994 *Phys. Rev. Lett.* **72** 2749
[15] Bracker A S, Yang M J, Bennett B R, Culbertson J C and Moore W J 2000 *J. Cryst. Growth* **220** 384
[16] Nguyen B M, Hoffman D, Huang E K, Bogdanov S, Delaunay P Y, Razeghi M and Tidrow M Z 2009 *Appl. Phys. Lett.* **94** 223506